Steady-State and Dynamic Modeling of Gas-Phase Polypropylene Processes Using Stirred-Bed Reactors

Neeraj P. Khare, Bruce Lucas, Kevin C. Seavey, and Y. A. Liu*

Honeywell Center of Excellence in Computer-Aided Design and SINOPEC/AspenTech Center of Excellence in Process Systems Engineering, Department of Chemical Engineering, Virginia Polytechnic Institute and State University, Blacksburg, Virginia 24061

Ashuraj Sirohi, Sundaram Ramanathan, Simon Lingard, Yuhua Song, and Chau-Chyun Chen

Aspen Technology, Inc., 10 Canal Park, Cambridge, Massachusetts 02141

This paper describes the development of a comprehensive model for the continuous gas-phase synthesis of polypropylene using stirred-bed reactors. The model considers the important issues of physical property and thermodynamic model selections, polymer properties, catalyst characterization, and reactor residence time, in addition to the traditional Ziegler−Natta polymerization kinetics. Model development involves fundamental chemical engineering principles and advanced software tools, Polymers Plus and Aspen Dynamics. We characterize a Ziegler−Natta catalyst by assuming the existence of multiple catalyst site types. The model contains a single set of kinetic and thermodynamic parameters that accurately predicts the polymer production rate, molecular weight, polydispersity index, and composition for both homopolymer and impact copolymer product grades from a large-scale commercial process. We demonstrate the application of our dynamic model and process control by comparing grade-transition strategies.

1. Introduction

1.1. Scope. The objective of this work is to describe the considerations and techniques used to develop a comprehensive model for a gas-phase polypropylene process using stirred-bed reactors. Our model focuses on the important issues of physical property and thermodynamic model selections, polymer properties, catalyst characterization, and reactor residence time, in addition to the traditional Ziegler−Natta polymerization kinetics. Physical properties, such as vapor and liquid densities, allow the model to accurately consider the reactor residence time and volumetric throughput. Phase equilibrium is important for modeling the flash vessels in the overhead recycle units. A robust model must account for these considerations. We also describe the characterization of a Ziegler−Natta catalyst containing multiple site types and provide iterative methodologies for determining the kinetic parameters.

A review of the representative models in the literature for the gas-phase polymerization of olefins reveals their primary focus on the polymerization kinetics alone, with inadequate consideration of the proper selection of the physical property and thermodynamic models and phase-equilibrium relationships. For example, Choi and Ray[1] presented a model for the gas-phase polymerization of propylene using continuous stirred-bed reactors. This model does not account for the effect of reactor temperature and pressure on the species densities, which is important for residence-time and throughput calculations. Their model employs the ideal-gas law for the vapor phase, which is generally not valid for the moderate-pressure vessels used in the gas-phase process. The model also assumes that the heat capacities of the monomer and polymer are constant over the temperature range of interest. These properties can change appreciably with relatively small changes in reactor temperature.

In another example, McAuley et al.[2] developed a model for the gas-phase polymerization of ethylene. As in the previous example, this model uses the ideal-gas law for the vapor phase and does not consider the effect of reactor conditions on species properties such as density or heat capacity. The user must supply parameters such as species concentrations and volumetric flow rates to use the model.

The selection of improper models for phase equilibrium and physical and thermodynamic properties does not seriously affect the utility of these models when used for specific values of feed composition and reactor conditions. However, it can severely limit the model applicability when the user attempts to change the reactor conditions or feed rates, as is commonly the case in industrial applications.

A model that correctly represents the phase equilibrium and physical and thermodynamic properties, in addition to the polymerization kinetics, is far more useful for exploring changes in feed composition and reactor conditions. This allows the user to model a particular system without the need to predetermine process variables such as densities, concentrations, and heat capacities. We are not aware of any such studies of this issue in the open literature prior to our current work.

1.2. Gas-Phase Processes Using Stirred-Bed Reactors. Gas-phase polymerization processes are widely used to produce polyolefins. They use either continuous-

* To whom correspondence should be addressed. Tel.: (540) 231-7800. Fax: (540) 231-5022. E-mail: design@vt.edu.

10.1021/ie030714t CCC: $27.50
Published on Web 01/27/2004

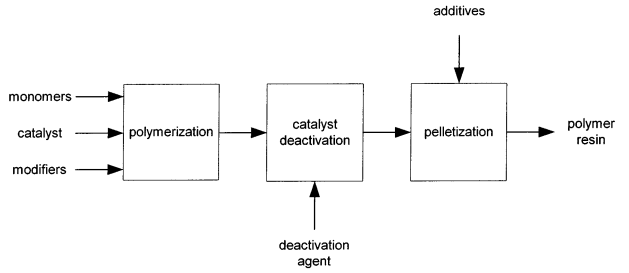

Figure 1. Simplified flowchart for the gas-phase polypropylene process.[8]

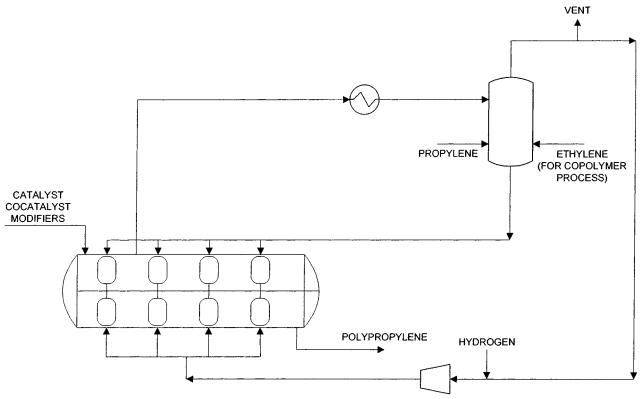

Figure 2. Example of a gas-phase polypropylene process using a stirred-bed reactor.[9]

flow stirred-bed or fluidized-bed reactors. Unlike slurry and solution processes, no liquid phase is present in the reactors, only vapor and solids. This makes the gas-phase process simpler, because there is no solvent or liquid monomer to separate from the polymer, purify, and recycle.[3]

The first commercial gas-phase processes for polyolefin production appeared in the late 1960s.[3] Amoco developed the first stirred-bed gas-phase reactor for polypropylene manufacture in the 1970s.[4−7] The gas-phase process involves the feeding of liquid monomer into the reactor, which evaporates upon entering. The system involves mechanical agitation, rather than fluidization. Companies that license polypropylene gas-phase processes include BP Amoco (Innovene), Dow (Unipol), Novolen Technology Holdings (Novolen), and Basell (Spheripol, Catalloy).

Figure 1 shows a simplified flowchart for the gas-phase production of polypropylene. Fresh monomer, catalyst, and modifiers (chain-transfer agent, etc.) are fed to the reactor section. Traditionally, the resulting polymer powder stream then undergoes catalyst deactivation. Additional modifiers are then added, depending on the intended use of the product. Finally, the polymer product is pelletized.[8]

The three general types of polypropylene produced in the gas-phase process are the homopolymer, random copolymer, and impact copolymer. The random copolymer contains small amounts of ethylene comonomer, and the impact copolymer is a mixture of homopolymer and copolymer that contains between 6 and 15 wt % ethylene comonomer.[8] Of these three types, we model the homopolymer and impact copolymer processes.

Figure 2 shows a simplified diagram of a typical gas-phase process using a stirred-bed reactor. The reactor temperature ranges from 57 to 77 °C, and the pressure ranges from 19 to 23 bar.[9] The reactor off-gas is condensed, flashed, and returned to the reactor. The vapor recycle enters at various points along the bottom of the bed at a low enough flow rate to avoid bed fluidization.[9] The liquid recycle is sprayed at various locations along the top of the reactor.[9] The vaporizing liquid absorbs most of the exothermic heat of polymerization, allowing for 10−15% conversion per pass to maintain a constant reactor temperature.[9] The polypropylene process uses a titanium-based catalyst and an aluminum-alkyl-based cocatalyst.[9] Examples are titanium tetrachloride ($TiCl_4$) and triethyl aluminum [$Al(C_2H_5)_3$], respectively.[10] Fresh propylene enters the process at the overhead flash unit. Ethylene also enters here, for copolymerization grades.[9] Fresh hydrogen, used for molecular-weight control, enters at the vapor recycle stream.[9] A small portion of the vapor recycle stream is vented to remove propane and ethane that accumulate in the recycle loop.[9] Tacticity control agents, fed with the catalyst, are commonly used to increase the isotactic content of the polypropylene.[11]

The reactor is horizontal and cylindrical and contains several zones that are sometimes separated by weirs.[9] The polymer exists as a powder, given that the reactor temperature remains well below the polypropylene melting point of 157 °C.[12] Paddles connected to a rotating shaft mildly agitate the powder.[9] For the impact-polymer process, two reactors are configured in series, and the second reactor incorporates the comonomer.

1.3. Modeled Process. We model a gas-phase polypropylene process using stirred-bed reactors on the basis of publicly available process patents[4−7] and research articles.[3,8,9,13] We validate the model using data from a commercial plant for four product grades.

1.4. Modeling Technology. The model incorporates fundamental chemical engineering principles and advanced software tools for both steady-state and dynamic process simulation. Modeling considerations include mass and energy balances, physical properties, phase equilibrium, polymerization kinetics, and reactor modeling. We use Polymers Plus and Aspen Dynamics to simulate the polypropylene process. Polymers Plus is a layered product built on top of Aspen Plus for polymer process simulation. It applies process modeling technology to a wide variety of polymerization processes. Aspen Dynamics converts steady-state process models to dynamic models that consider time-dependent effects and control schemes.

Polymers Plus includes the characterization of polymers and tracking of their structural properties throughout the flowsheet, phase equilibrium for polymer systems, polymerization kinetics, and reactor modeling. It uses a segment-based approach for computing the physical properties of polymer species. By considering a polymer chain as a series of segments whose structures are well-defined, Polymers Plus can model the polymer properties that commonly vary with time and location (reactor 1 or reactor 2) in a synthesis process. This technique permits the modeling of properties such as molecular weight and copolymer composition and can account for the fact that most polymer products contain an ensemble of molecules having a distribution of chain lengths. It facilitates the use of group-contribution methods for the estimation of properties such as heat capacity, density, and melt- and glass-transition temperatures when no data are available. Polymers Plus can also incorporate subroutines for user-defined correlations for polymer properties such as density and melt flow rate.

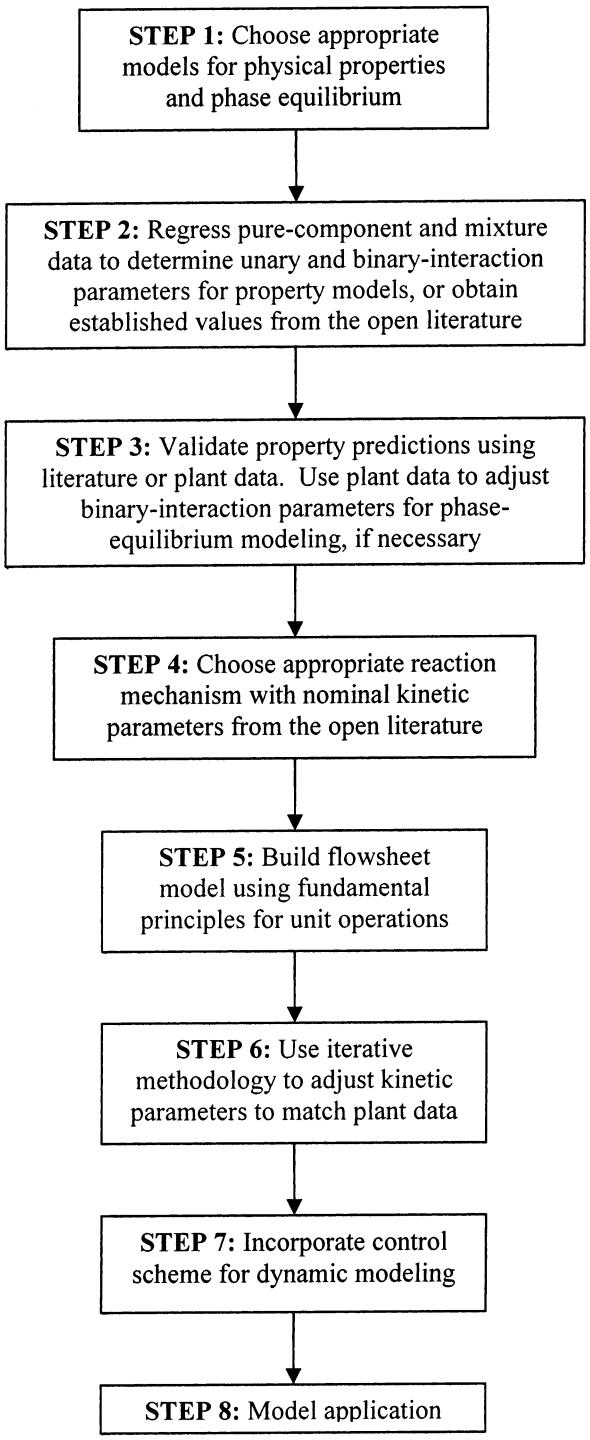

Figure 3. Procedure for developing the polypropylene process model.

We export the steady-state model from Polymers Plus to Aspen Dynamics and incorporate appropriate control schemes to simulate a polymer grade change. The successful development and validation of the model illustrates the powerful modeling and predictive capabilities of this integrated software package.

1.5. Modeling Methodology. Proper consideration of the polymerization mechanism and kinetics is essential to any polymer synthesis model. However, a robust model must also accurately account for physical properties and phase equilibrium. Figure 3 presents a flowchart for the procedure we follow to develop and validate the polypropylene process model. This figure shows how we integrate the key elements of our model, including physical and thermodynamic properties, phase equilibrium, polymerization kinetics, and flowsheet simulation. These modeling elements are identical to those key components required by most commercial process simulation software tools, that is, components, properties, streams, blocks, flowsheet, and reactions. We illustrate the accuracy of the model using the numerous figures and tables that compare model predictions to experimental data.

In developing our model, we first choose physical-property and thermodynamic models that permit accurate descriptions of the density, enthalpy, phase-equilibrium behavior, and other properties for each species in the system. Accurate density modeling permits proper considerations for equipment sizing and capacity. Enthalpy predictions allow for accurate heat-balance computations. Phase equilibrium is important for predicting the monomer and hydrogen concentrations in the polymer phase and for the overhead condensers that partially liquefy the propylene mixture before returning to the reactor. Section 2 describes the equation of state based on the perturbed-chain statistical associating fluid theory (PC−SAFT EOS) that we use for modeling these properties.

Next, we establish pure-component and binary-interaction parameters for the physical-property and thermodynamic models. This can be accomplished in two ways. The simplest method is to obtain values from the open literature. If we take this approach, we must make sure that the parameters were determined using experimental data that were obtained under conditions close to the conditions in the modeled process. If this is not the case, or if parameters are not available in the open literature, we must obtain values by regressing experimental data. We must then validate the property predictions by comparing them to experimental or plant data. Sections 2.3 and 2.4 report the parameter values and sources we use, as well as validation plots.

In section 3, we establish the polymerization kinetics for the Ziegler−Natta-catalyzed system. We obtain a nominal set of kinetic parameters from the open literature.

We develop the process model by considering fundamental mass and energy balances for all of the relevant unit operations. In addition to the reactors, we include heat exchangers, flash vessels, pumps, and compressors for the recycle system.

After considering flow rates and compositions for fresh-feed streams, as well as conditions for unit operations, we use the process model to adjust kinetic parameters to match the plant data for process targets. These include polymer molecular weight, composition, production rate, and monomer conversions. We establish the kinetics for a Ziegler−Natta catalyst with multiple site types by deconvoluting gel-permeation chromatography (GPC) data for the polymer. Because many of the reactions in the polymerization mechanism are coupled, we must use iterative techniques to obtain a final set of kinetic parameters that allow the model to match plant data. Finally, we validate the model by comparing predictions with data for four polymer grades.

2. Physical Properties and Thermodynamic Modeling

2.1. Introduction. We use the PC−SAFT EOS to model the physical and thermodynamic properties for

the polypropylene process. EOS models are appropriate for systems at moderate to high pressures. Reactor pressures for the gas-phase polypropylene process range from 20 to 30 bar. Equations of state also provide unified property predictions across the vapor−liquid transition. The PC−SAFT model was designed specifically for polymer systems and is suitable for the modeled process.

In the next section, we provide additional details about the PC−SAFT EOS. We then discuss pure-component and mixture properties, respectively, in sections 2.3 and 2.4.

2.2. PC−SAFT EOS. Gross and Sadowski[14] recently developed the PC−SAFT EOS, which is an extension of the well-known SAFT EOS.[15−17] As with other EOS based on perturbation theory, the PC−SAFT model expresses the residual Helmholtz energy as a sum of two contributions

$$a^{\text{res}} = a^{\text{ref}} + a^{\text{pert}} \tag{1}$$

where a^{res} is the molar residual Helmholtz energy and a^{ref} and a^{pert} are the reference and perturbation contributions, respectively. The reference term considers a fluid consisting of hard-sphere chains as a reference for the perturbation theory, and the perturbation term incorporates the attractive forces between the chains. The primary difference between the PC−SAFT and SAFT models is in the perturbation term. The SAFT model uses hard spheres, not hard-sphere chains, as a reference fluid for the perturbation contribution. The use of hard-sphere chains allows the PC−SAFT EOS to account for the connectivity of segments that comprise the chains when considering the attractions between species, resulting in a more realistic description of the thermodynamic behavior of mixtures of chainlike molecules. The PC−SAFT EOS is valid for both small molecules and chainlike polymers. Gross and Sadowski demonstrated that the PC−SAFT predictions for VLE are superior to those of the SAFT model. PC−SAFT also performs better than the Peng−Robinson EOS for binary mixtures of small molecules.[14]

The resulting equation of state expresses the compressibility as follows

$$z = z^{\text{id}} + z^{\text{ref}} + z^{\text{pert}} \tag{2}$$

where z^{id} is the ideal contribution to the compressibility, with a value of unity, and z^{ref} and z^{pert} are the reference and perturbation contributions, respectively,corresponding to those described above.

The PC−SAFT EOS requires three pure-component parameters for each pure species. It has an optional binary interaction parameter that can be used to correlate phase-equilibrium behavior. We provide the parameters used in the model in the following sections.

2.3. Pure-Component Properties. Table 1 lists the components we include in the model. As described in section 1.3, we use a segment-based approach for the polymer species. We must therefore consider segment species corresponding to each type of monomer that comprises the polymer.

2.3.1. PC−SAFT Pure-Component Parameters. Table 2 lists the pure-component parameters for the PC−SAFT model and the corresponding sources for the parameters or experimental data. The parameter σ is a characteristic diameter for the segments of a given species. The parameter ϵ is a segment energy parameter. The parameter m serves as a characteristic chain length. For polymer species, we use r, the ratio of m to the number-average molecular weight

Table 1. Components Used in the Model

species	function
titanium tetrachloride	catalyst
triethyl aluminum	cocatalyst
propylene	monomer
propylene segment	monomer segment
ethylene	comonomer
ethylene segment	comonomer segment
polypropylene	polymer
hydrogen	chain-transfer agent
tacticity control agent	tacticity control agent
ethane	impurity
propane	impurity

Table 2. Pure-Component Parameters for the PC−SAFT EOS

species	m	σ (Å)	ϵ/k_B[a] (K)	r (mol/g)	ref
hydrogen	0.8285	2.973	12.53	−	18
ethylene	1.559	3.434	179.4	−	19
ethane	1.607	3.521	191.4	−	14
propylene	1.960	3.536	207.2	−	14
propane	2.002	3.618	208.1	−	14
polypropylene	−	4.147	298.6	0.0253	20
polyethylene	−	4.022	252.0	0.0263	14
tacticity control agent	25.00	2.668	198.8	−	−
catalyst	25.00	2.668	198.8	−	−
cocatalyst	25.00	2.668	198.8	−	−

[a] k_B is the Boltzmann's constant, 1.38×10^{-23} J/K.

$$r = \frac{m}{M_n} \tag{3}$$

in place of the segment number m. This is more convenient because the polymer molecular weight is often unknown until after the polymer is produced.

Generally, we regress data along the saturation curve to obtain pure-component parameters for conventional species. For polymer species, which are essentially nonvolatile, we use data for liquid density[20] and liquid heat capacity.[21] Because ethylene is near the supercritical state (T_c = 9.25 °C, P_c = 50.4 bar),[22] we use additional density data in the supercritical region to obtain pure-component parameters. For hydrogen, we fit only the supercritical density data for the ranges 25−170 °C and 1−200 bar because the critical temperature of hydrogen is well below the conditions used in the modeled process. In general, we choose values for the tacticity control agent, catalyst, and cocatalyst so that these species remain in the liquid phase and are miscible with the key component in the streams where no polymer exists. In particular, we use a relatively high value of 25 for the parameter m, which primarily controls the calculated vapor pressure in the PC−SAFT EOS.

2.3.2. Heat Capacity. We compute the heat capacity for each species by summing the ideal-gas and EOS contributions

$$C_p(T,P) = C_p^{\text{ig}}(T) + \Delta C_p(T,P) \tag{4}$$

where $C_p^{\text{ig}}(T)$ is the ideal-gas term, evaluated at the system temperature, and $\Delta C_p(T,P)$ is the departure

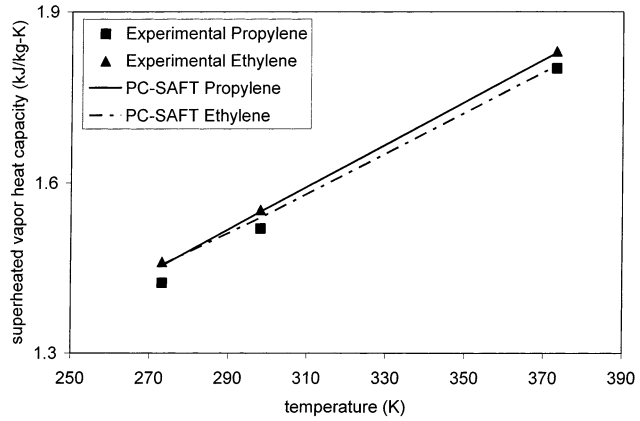

Figure 4. Comparison of experimental data with PC−SAFT predictions for the heat capacities of superheated propylene and ethylene vapor. Data are from Beaton and Hewitt.[25]

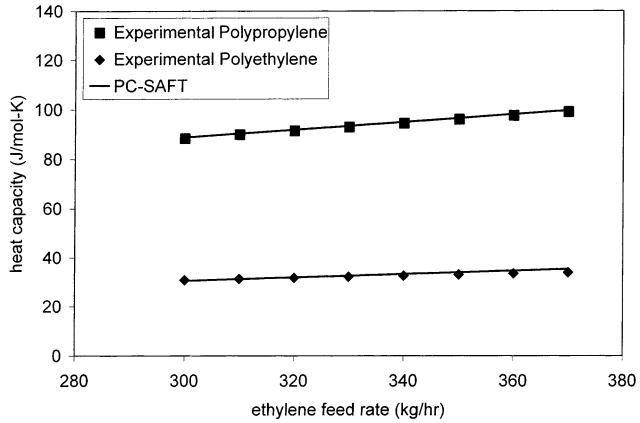

Figure 5. Comparison of experimental data with PC−SAFT predictions for the heat capacities of polypropylene and polyethylene. Data are from Gaur and Wunderlich.[21,24]

Table 3. Parameters for the Ideal-Gas Heat-Capacity Model

species	*A* (J/kmol·K)	*B* (J/kmol·K^2)	*C* (J/kmol·K^3)	*D* (J/kmol·K^4)	ref
hydrogen	27 140	9.274	-1.381×10^{-2}	7.645×10^{-6}	23
ethylene	3806	156.6	-8.348×10^{-2}	1.755×10^{-5}	23
ethane	5409	178.1	-6.938×10^{-2}	8.713×10^{-6}	23
propylene	3710	234.5	−0.116	2.205×10^{-5}	23
propane	−4224	306.3	−0.1586	3.215×10^{-5}	23
polypropylene	42 960	152.9	2.392×10^{-5}	0	21
polyethylene	10 100	68.22	0	0	24

term, evaluated by the EOS at the system temperature and pressure. Because we use an ideal gas as a reference state for all species, we consider a hypothetical ideal-gas heat capacity for the nonvolatile species, such as the polymer and catalyst. We compute the ideal-gas heat capacity using a polynomial

$$C_p^{ig}(T) = A + BT + CT^2 + DT^3 \qquad (5)$$

where *A*, *B*, *C*, and *D* are adjustable parameters. Table 3 lists the parameters used for each species. We neglect the heat capacity of the catalyst and cocatalyst, they are present only in trace amounts. Figure 4 compares our model predictions with experimental data for the heat capacities of propylene and ethylene. Figure 5 provides a similar comparison for the heat capacities of polypropylene and polyethylene. The fits are excellent.

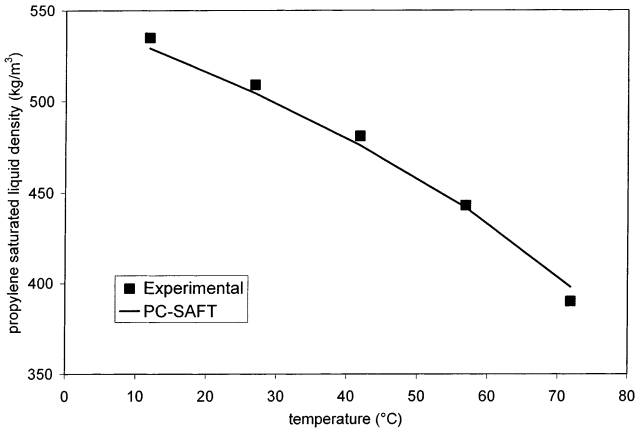

Figure 6. Comparison of experimental data with PC−SAFT predictions for the saturated liquid density of polypropylene. Data are from Beaton and Hewitt.[25]

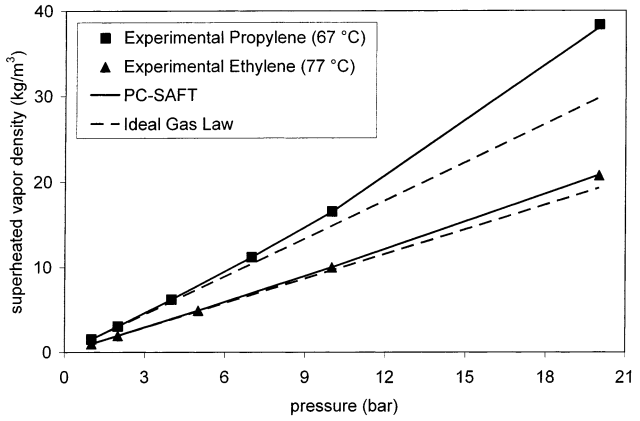

Figure 7. Comparison of experimental data with PC−SAFT predictions for the superheated vapor density of propylene and ethylene. The ideal-gas law is unable to describe the propylene density at reactor conditions. Data are from Beaton and Hewitt.[25]

2.3.3. Density. Accurate density predictions are important for modeling equipment capacity and throughput. Incorrect condensed-phase densities can lead to inaccurate reactor residence times, which affect most polymer properties. Vapor-phase densities must be correct to properly consider volumetric throughput for the overhead recycle units. The PC−SAFT EOS gives an excellent description of the vapor and liquid densities of the species in the polypropylene process.

Figure 6 shows the saturated liquid density for propylene. Figure 7 shows the superheated vapor densities for propylene and ethylene. In the latter figure, we include comparisons with the ideal-gas law to illustrate that, at the reactor conditions, the ideal-gas law is not capable of accurately describing the density of superheated propylene. The density error can be more than 25%, thus negatively impacting the residence-time calculations. Figure 8 shows the density for polypropylene. The PC−SAFT EOS represents the density of each species well.

2.3.4. Vapor Pressure. An accurate prediction of the vapor pressure is important for the overhead flash vessel. The amount of liquid propylene that recycles to the reactor dictates the conversion per pass, because the vaporization of the propylene absorbs most of the heat of polymerization. Figure 9 shows the vapor pressure for propylene. The PC−SAFT EOS prediction agrees well with the experimental data.

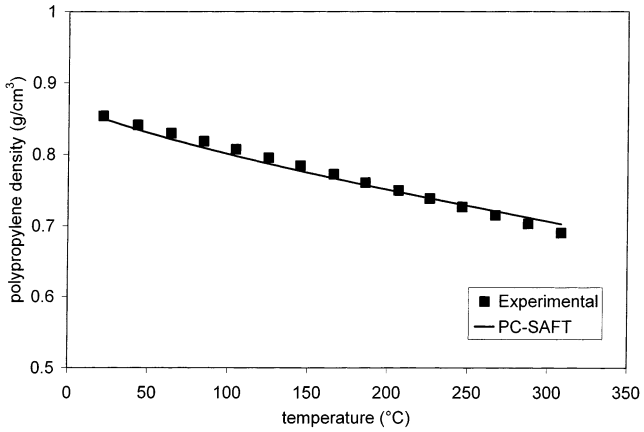

Figure 8. Comparison of experimental data with PC−SAFT predictions for polypropylene density. Data are from Zoller.[20]

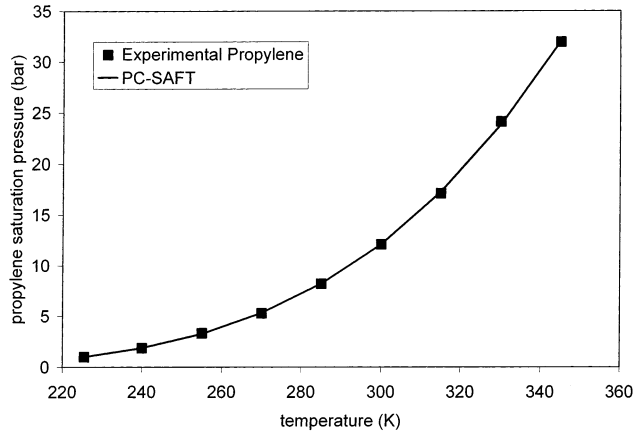

Figure 9. Comparison of experimental data with PC−SAFT predictions for propylene vapor pressure. Data are from Beaton and Hewitt.[25]

2.3.5. Heat of Vaporization. The reaction mixture remains at a constant temperature because of the evaporation of the liquid propylene mixture fed to the reactor. We require accurate modeling of the heats of vaporization of the major components to obtain an accurate heat balance. We compute the heat of vaporization by taking the difference between the calculated values of the pure-component enthalpies of the vapor and liquid at a given temperature and pressure

$$\Delta H_i^{\mathrm{vap}}(T,P) = H_i^{\mathrm{v}}(T,P) - H_i^{\mathrm{l}}(T,P) \qquad (6)$$

Figure 10 shows the heats of vaporization of propylene and ethylene. The PC−SAFT EOS accurately predicts the experimental values in both cases.

2.4. Mixture Properties. VLE predictions are important in the overhead condensers for recycle to the reactors. Inaccurate solubility predictions can cause trace components, such as hydrogen, to either accumulate in or disappear from the recycle loop. In general, we initially do not use binary-interaction parameters for the PC−SAFT EOS. Data from the open literature tend to be too scarce to yield accurate values. If necessary, we can use plant data to regress binary interaction parameters between key species.

Figures 11 and 12 show the solubilities of ethylene and hydrogen, respectively, in propylene. The PC−SAFT EOS performs well in both cases. We do not include

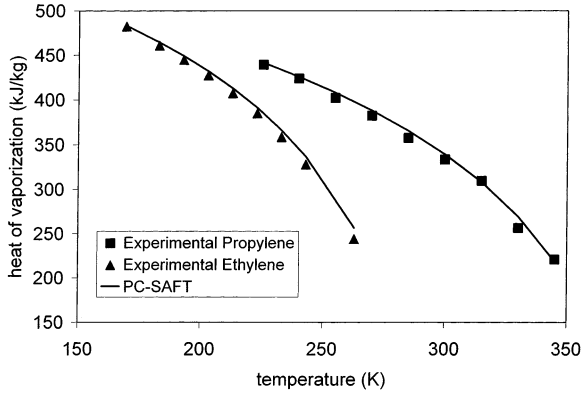

Figure 10. Comparison of experimental data with PC−SAFT predictions for the heats of vaporization of propylene and ethylene. Data are from Beaton and Hewitt.[25]

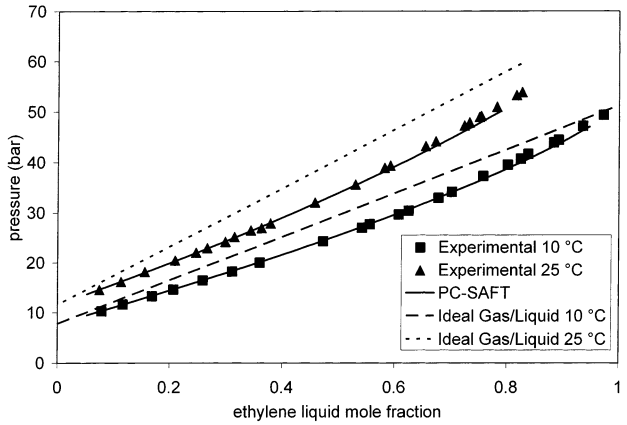

Figure 11. Comparison of experimental data with PC−SAFT predictions for the solubility of ethylene in propylene. Data are from Ohgaki et al.[26]

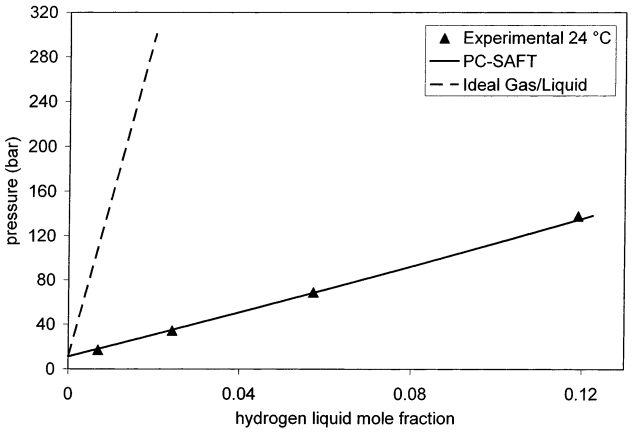

Figure 12. Comparison of experimental data with PC−SAFT predictions for the solubility of hydrogen in propylene. Data are from Williams and Katz.[27]

binary-interaction parameters in the model because the solubility predictions are sufficiently accurate. This approach is in agreement with literature reports indicating that the PC−SAFT EOS is accurate with binary-interaction parameters set to zero for mixtures of nonassociating species.[14] An assumption of ideal gas/liquid produces erroneous results, particularly in the case of hydrogen solubility in liquid propylene.

2.5. Polymer Properties. 2.5.1. Heat of Polymerization. We compute the heat of polymerization by considering the difference between the enthalpies of

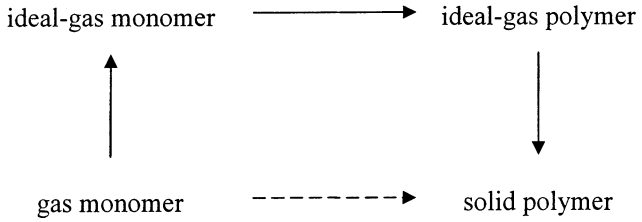

Figure 13. Method for computing the heat of propylene polymerization for the equation-of-state approach.[28]

Table 4. Comparison of PC−SAFT Predictions for the Heat of Propylene Polymerization with an Experimental Value of 24.84 kcal/mol at 25 °C[28]

T (°C)	P (bar)	$H_{\text{propylene}}$ (kcal/mol)	$H_{\text{polypropylene}}$ (kcal/mol)	ΔH_f (kcal/mol)
25	20	4.05	−20.73	−24.78
35	20	4.29	−20.46	−24.75
45	20	4.50	−20.19	−24.69
55	20	4.71	−19.92	−24.63
65	20	4.91	−19.64	−24.55
75	20	5.11	−19.37	−24.48

gaseous propylene and solid polymer (propylene segment) at the same conditions[28]

$$C_3H_6(g) \rightarrow \frac{1}{n}(C_3H_6)_n(s) \tag{7}$$

where n is the number of propylene segments in the polymer. Figure 13 illustrates the method used to compute the heat of polymerization. We use the equation of state to compute each transition along the path.

Table 4 compares PC−SAFT predictions with an experimental value for the heat of polymerization, ΔH_f, of −24.84 kcal/mol at 25 °C.[28] The computed values compare favorably with the literature value.

2.5.2. Molecular Weight from Method of Moments. We use the method of moments (population balance) to track the leading moments of the molecular-weight distribution of the polymer. The moments are sums of the concentrations of polymer species weighted by chain length. The moment expression for live polymer chains is

$$\mu_i = \sum_{n=1}^{\infty} n^i[P_n] \tag{8}$$

where μ_i is the ith moment for live (growing) chains and $[P_n]$ is the concentration of polymer chains containing n segments. The expression for bulk (live plus dead) chains is

$$\lambda_i = \sum_{n=1}^{\infty} n^i([P_n] + [D_n]) \tag{9}$$

where λ_i is the ith moment for all polymer chains and $[D_n]$ is the concentration of dead (inactive) polymer chains. When the rate equations are summed over all n, they become functions of these moments, yielding a small number of closed expressions. Arriola has provided a detailed description and derivations of the method of moments for addition polymerizations.[29]

The zeroth, first, and second moments are sufficient for the computation of common molecular-weight properties of polypropylene. These include the number-average molecular weight (M_n), the weight-average molecular weight (M_w), and the polydispersity index (PDI)

$$M_n = \text{MW}_{\text{seg}} \frac{\lambda_1}{\lambda_0} \tag{10}$$

$$M_w = \text{MW}_{\text{seg}} \frac{\lambda_2}{\lambda_1} \tag{11}$$

$$\text{PDI} = \frac{M_w}{M_n} = \frac{\lambda_2\lambda_0}{\lambda_1^2} \tag{12}$$

where MW_{seg} is the molecular weight of the polymer segments. For copolymers, we use a molar average of each segment type

$$\text{MW}_{\text{seg}} = X_{\text{propylene}}\text{MW}_{\text{propylene}} + X_{\text{ethylene}}\text{MW}_{\text{ethylene}} \tag{13}$$

where $X_{\text{propylene}}$ and X_{ethylene} are the mole fractions of propylene and ethylene segments, respectively, in the polymer; $\text{MW}_{\text{propylene}}$ is 42.08 g/mol; and $\text{MW}_{\text{ethylene}}$ is 28.05 g/mol.

3. Reactor Modeling

3.1. Using CSTRs in Series. During steady-state operation, the polymer level remains constant along the reactor length.[9] The paddles along the reactor agitate the polymer only mildly, and the solids are not fluidized.[9] The polymer phase essentially experiences plug-flow conditions along the reactor length. Plug flow can be simulated by using several continuous stirred-tank reactors (CSTRs) configured in series.[30] Experimental studies on the residence-time distribution (RTD) of polymers produced in horizontal stirred-bed reactors suggest that the polymer RTD is equivalent to that produced by three to five CSTRs.[9] Figure 14 compares the actual reactor to this modeling assumption. In our model, we use four CSTRs to represent the stirred-bed reactor. Other modelers have used this approach as well.[13] Each CSTR receives liquid and vapor recycled from the overhead condenser, which includes fresh monomer and hydrogen. Only the first CSTR receives fresh catalyst and cocatalyst. The temperature and pressure are the same for all zones.

The concept of residence time is significantly different between this situation and that for multiple CSTRs in series. Furthermore, a residence-time calculation requires knowledge of the volumetric holdup in the reactor. This cannot be measured very accurately because the paddles are always agitating the polymer and there is a void fraction associated with the solid phase. We therefore do not use residence time as a simulation target in the model and instead use reactor mass holdup. In the simulation, we constrain the CSTRs to the same polymer mass to maintain the same level along the bed length. This results in monotonically decreasing residence times for the four CSTRs corresponding to a given stirred-bed reactor, which conforms to reported experimental results.[9]

3.2. Phase Equilibrium. The reaction mixture in the gas-phase process contains only solid and vapor. The liquid recycle essentially vaporizes instantly upon introduction into the reactor. The reactor temperature is well below the polymer melting point. We treat the solid polymer as a pseudo-liquid in the VLE calculations. As shown in Figure 8, this approach does not diminish the

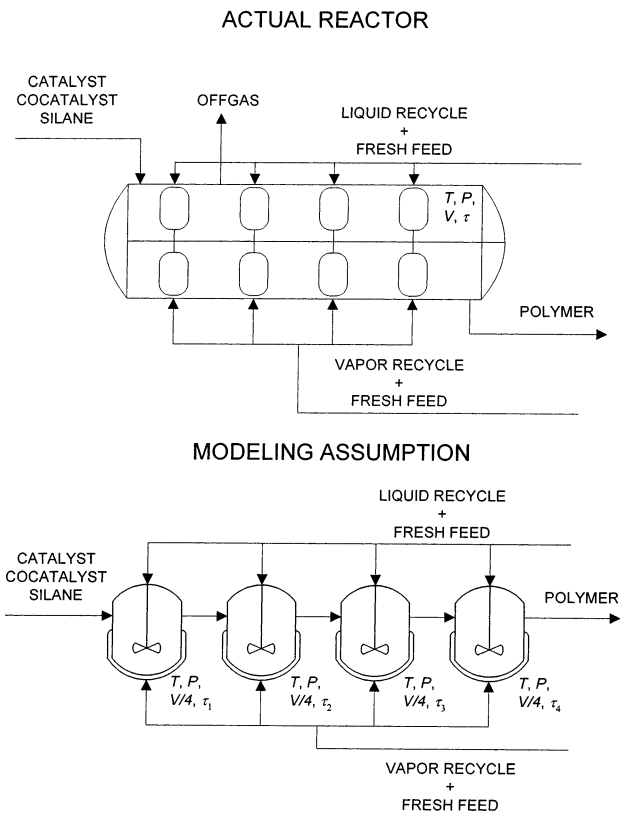

Figure 14. Comparison of the actual reactor with the modeling assumption of four CSTRs in series.

accuracy of the predictions of the polypropylene density because we use density data to determine the PC−SAFT parameters for the polymer.

4. Polymerization Kinetics

4.1. Introduction. Many studies have been conducted on the kinetics of olefin polymerization using Ziegler−Natta catalysts.[31−36] These catalysts tend to produce polymers with broad molecular-weight distributions (MWDs). There are traditionally two main schools of thought on the reason why this occurs. One argument is that mass- and heat-transfer resistances lead to a broadening of the MWD. The other argument is that there are multiple site types, each with its own relative reactivity. Under most polymerization conditions, however, the effect of multiple site types is more important than that of transport resistances.[37] We assume that each site type produces polymer with a most-probable MWD. The resulting composite polymer produced by all of the site types together has a broad MWD.

We develop a kinetic model for a Ziegler−Natta catalyst containing multiple site types to describe the polymer production rate, molecular weight and its distribution, and copolymer composition. Sections 4.2 and 4.3 outline the homo- and copolymerization kinetic schemes. Section 4.4 describes the process used to determine kinetic parameters for the model.

4.2. Homopolymerization Kinetic Scheme. We use a subset of the Ziegler−Natta reactions described in refs 31−36. Table 5 lists the homopolymerization reactions. These reactions allow the model to describe the polymer properties for each grade. We describe these reactions next.

4.2.1. Catalyst Activation. For a typical Ziegler−Natta catalyst, a cocatalyst, such as triethyl aluminum,[10] is usually used to activate the sites on a titanium catalyst

Table 5. Reaction Subset Used for Homopolymerization Kinetics

reaction number	description
1	catalyst site activation
2	chain initiation
3	chain propagation
4	chain transfer
5	catalyst site deactivation

$$\mathrm{CAT}_i + \mathrm{COCAT} \xrightarrow{k_{\mathrm{act},i}} \mathrm{P}_{0,i} \tag{14}$$

where $k_{\mathrm{act},i}$ is the rate constant for the activation of catalyst site type i by cocatalyst. Active sites undergo initiation and subsequent propagation by monomer to form the polymer chains. Because Ziegler−Natta catalysts tend to activate quickly, we use a relatively high rate constant for catalyst activation. One could also use activity profiles from semibatch reactor experiments to determine a value for the rate constant.

Hydrogen is known to enhance catalyst activity in gas-phase polypropylene processes.[36] The reaction is

$$\mathrm{CAT}_i + \mathrm{H}_2 \xrightarrow{k_{\mathrm{acth},i}} \mathrm{P}_{0,i} \tag{15}$$

where $k_{\mathrm{acth},i}$ is the rate constant for activation of catalyst site type i.

The model contains a "max sites" parameter representing the number of catalyst sites per unit mass of catalyst. Parameter values usually range from 1.0×10^{-5} to 1.0×10^{-3} mol of sites per gram of catalyst (inverse of catalyst molecular weight). The utility of the max sites parameter is that it proportionally scales the rates of the reactions involving catalyst sites (propagation, chain transfer, etc.), allowing us to adjust the production rate without affecting the molecular weight or copolymer composition.

4.2.2. Chain Initiation. Monomer (M) can initiate chain growth by reacting with an active site

$$\mathrm{P}_{0,i} + \mathrm{M} \xrightarrow{k_{\mathrm{ini},i}} \mathrm{P}_{1,i} \tag{16}$$

where $k_{\mathrm{ini},i}$ is the rate constant for chain initiation at site type i and $\mathrm{P}_{1,i}$ is an initiated catalyst site of type i with a single monomer attached to it. Because we cannot experimentally determine individual values for chain initiation and propagation for a given monomer, we set their rate constants equal.

4.2.3. Chain Propagation. Chain propagation is the mechanism by which the polymer chains grow. Additional monomer adds to existing chains at the active catalyst sites according to the reaction

$$\mathrm{P}_{n,i} + \mathrm{M} \xrightarrow{k_{\mathrm{p},i}} \mathrm{P}_{n+1,i} \tag{17}$$

where $k_{\mathrm{p},i}$ is the rate constant for chain propagation at site type i and $\mathrm{P}_{n,i}$ and $\mathrm{P}_{n+1,i}$ are polymer chains associated with site type i of lengths n and $n+1$, respectively. An increase in the rate constants for propagation yields a linear increase in the polymer molecular weight. The reaction in eq 17 accounts for the total amount of polymer produced, including both isotactic and atactic formations.

We also include a propagation reaction to account for the small amount of atactic polymer produced

$$P_{n,i} + M \xrightarrow{k_{pa,i}} P_{n+1,i} \quad (18)$$

where $k_{pa,i}$ is the rate constant for atactic chain propagation at site type i. This reaction does not affect the total amount of polymer produced or the monomer conversions. We compute the atactic fraction by dividing the amount of polymer produced via total propagation by that produced via atactic propagation

$$\text{atactic fraction} = \frac{\text{rate of atactic propagation}}{\text{rate of total propagation}} \quad (19)$$

4.2.4. Chain Transfer. In chain transfer, a species, such as hydrogen or monomer, disengages the polymer chain from an active site, yielding a dead polymer chain. The empty catalyst site is then capable of producing a new polymer chain. This process limits the molecular weight of the polymer. Hydrogen is used for controlling the molecular weight of the polypropylene produced in the gas-phase process.[9]

Hydrogen reacts with an active catalyst site to disengage the polymer chain, rendering the chain inactive (dead), and leaving an empty catalyst site

$$P_{n,i} + H_2 \xrightarrow{k_{th,i}} D_n + P_{0,i} \quad (20)$$

where $k_{th,i}$ is the rate constant for chain transfer to hydrogen corresponding to site type i and D_n is an inactive polymer chain.

Chain transfer to monomer yields a dead chain and an initiated catalyst site

$$P_{n,i} + M \xrightarrow{k_{tm,i}} D_n + P_{1,i} \quad (21)$$

where $k_{tm,i}$ is the rate constant for chain transfer to monomer corresponding to site type i. We adjust the rate constants for these two chain-transfer reactions to match the polymer number-average molecular weight, M_n.

4.2.5. Catalyst Deactivation. The catalyst sites (both vacant and occupied) can undergo spontaneous deactivation

$$P_{0,i} \xrightarrow{k_{ds,i}} DCAT_i \quad (22)$$

$$P_{n,i} \xrightarrow{k_{ds,i}} D_n + DCAT_i \quad (23)$$

where $k_{ds,i}$ is the rate constant for deactivation for site type i and $DCAT_i$ is a deactivated catalyst site of type i. An increase in this rate constant leads to a decrease in polymer production rate. It can also affect the polymer number-average molecular weight (M_n) if the rate of chain transfer is low.

The tacticity control agent can also participate in catalyst site deactivation.[11] The corresponding reaction is

$$P_{0,i} + TCA \xrightarrow{k_{dtca,i}} DCAT_i \quad (24)$$

$$P_{n,i} + TCA \xrightarrow{k_{dtca,i}} D_n + DCAT_i \quad (25)$$

where TCA is the tacticity control agent and $k_{dtca,i}$ is the rate constant for deactivation of site type i by the TCA. Theoretically, the TCA deactivates a portion of the catalyst sites that produce atactic polymer.[11] We account for this in the multisite model, described in section 4.4.4.

4.3. Copolymerization Kinetic Scheme. The introduction of comonomer disrupts the regularity along the polymer chain, reducing the polymer crystallinity and density. The modeled process uses ethylene as the comonomer. We include cross-propagation reactions to account for the incorporation of comonomer. This approach follows the terminal model, where the rate of propagation for a specific monomer species depends on the last monomer species added to the chain, which is the active segment. For a two-monomer system, we extend eq 17 as follows

$$P^1_{n,i} + M_1 \xrightarrow{k^{11}_{p,i}} P^1_{n+1,i} \quad (26)$$

$$P^1_{n,i} + M_2 \xrightarrow{k^{12}_{p,i}} P^2_{n+1,i} \quad (27)$$

$$P^2_{n,i} + M_1 \xrightarrow{k^{21}_{p,i}} P^1_{n+1,i} \quad (28)$$

$$P^2_{n,i} + M_2 \xrightarrow{k^{22}_{p,i}} P^2_{n+1,i} \quad (29)$$

where $P^j_{n,i}$ is a polymer chain of length n associated with site type i that has an active segment corresponding to monomer of type j and $k^{jk}_{p,i}$ is the rate constant for propagation associated with site type i for a monomer of type k adding to a chain with an active segment of type j.

Because the amount of ethylene comonomer is small relative to the amount of propylene, there are far fewer chains with ethylene active segments than with propylene active segments. As a result, the primary reaction affecting propylene consumption is the propagation reaction involving propylene monomer and chains with propylene as the active segment. Similarly, the main reaction affecting ethylene conversion is the propagation reaction involving ethylene and chains with propylene as the active segment.

As with the propagation reactions, we also expand the chain-initiation and chain-transfer reactions for the copolymer case. For chain initiation

$$P_{0,i} + M_1 \xrightarrow{k^1_{ini,i}} P^1_{1,i} \quad (30)$$

$$P_{0,i} + M_2 \xrightarrow{k^2_{ini,i}} P^2_{1,i} \quad (31)$$

where M_j represents monomer of type j and $k^j_{ini,i}$ is the rate of chain initiation for monomer j at site type i.

For chain transfer to hydrogen

$$P^1_{n,i} + H_2 \xrightarrow{k^1_{th,i}} D_n + P_{0,i} \quad (32)$$

$$P^2_{n,i} + H_2 \xrightarrow{k^2_{th,i}} D_n + P_{0,i} \quad (33)$$

where $k^j_{th,i}$ is the rate constant for chain transfer to hydrogen associated with a chain ending with a monomer unit of type j at site type i.

For chain transfer to monomer

$$P^1_{n,i} + M_1 \xrightarrow{k^{11}_{tm,i}} D^1_{n,i} + P^1_{1,i} \quad (34)$$

$$P^1_{n,i} + M_2 \xrightarrow{k^{12}_{tm,i}} D^1_{n,i} + P^2_{1,i} \quad (35)$$

$$P^2_{n,i} + M_1 \xrightarrow{k^{21}_{tm,i}} D^2_{n,i} + P^1_{1,i} \quad (36)$$

$$P^2_{n,i} + M_2 \xrightarrow{k^{22}_{tm,i}} D^2_{n,i} + P^2_{1,i} \quad (37)$$

where $k^{jk}_{tm,i}$ is the rate constant for chain transfer to monomer of type k reacting with a chain with a terminal segment type j that is associated with catalyst site type i.

4.4. Determination of Kinetic Parameters. 4.4.1. Introduction. In this section, we describe how to use plant data to determine kinetic parameters for the gas-phase polymerization of propylene using a Ziegler−Natta catalyst. Because the polymerization reactions are highly coupled, adjusting a single kinetic parameter can affect several simulation variables. This makes parameter determination difficult. To simplify this process, we follow a procedure similar to that used recently for modeling an industrial slurry high-density polyethylene (HDPE) process with a Ziegler−Natta catalyst.[38] Using a two-step process, we establish a set of kinetic parameters that allows the model to accurately predict the polymer properties for several grades of polypropylene. In the first step, we assume that the catalyst contains a single site type. This allows us to model the value of M_n but not M_w, or equivalently, PDI. In the second step, we assume the catalyst has multiple site types. We deconvolute GPC data for the polymer to determine the number of site types required to accurately describe the MWD, as well as the relative amount of polymer, and the corresponding M_n, produced by each site type. It is much simpler to use this two-step process than to determine all of the parameters at once. Table 6 lists the simulation targets for the single- and multisite models.

Section 4.4.2 describes parameter determination for the single-site approach. Section 4.4.3 provides a brief overview of the deconvolution method and the software used. Section 4.4.4 details the multisite model. We manually implemented iterative methodologies to adjust the kinetic parameters to match plant data in both the single- and multisite approaches.

4.4.2. Single-Site Kinetic Model. A kinetic model for a catalyst with a single site type allows for the modeling of all simulation targets and polymer properties except the polymer PDI. It has significantly fewer kinetic parameters than a multisite model. Because we must use iterative schemes to adjust the kinetic parameters to match plant data, this reduction greatly facilitates the process. Another advantage is that we can use the single-site parameters as the initial values in the multisite model.

Table 7 lists a nominal set of kinetic parameters obtained from the open literature. We used an initial value of 0.0002 mol of sites/mol of Ti.[31] Using the Table 7 values as initial values, we manually step through the methodology outlined in Figure 15 to adjust the kinetic parameters to match plant data. The simulation targets for the single-site model appear in Table 6.

Table 6. Simulation Targets for Models for Catalysts with Single and Multiple Site Types

model for single-site catalyst	model for multisite catalyst
polymer production rate	polymer production rate
polymer M_n	polymer M_n
ethylene content	ethylene content
isotacticity (homopolymer)	isotacticity (homopolymer)
	relative polymer production at each site type
	polymer M_n at each site type
	polymer PDI

Table 7. Nominal Set of Kinetic Parameters for the Single-Site Model

reaction	reactant 1	reactant 2	k^a	ref	comments
cat-act	catalyst	cocatalyst	1	32	
cat-act	catalyst	hydrogen	1		*b*
chain-ini	catalyst	propylene	0.014		*c*
chain-ini	catalyst	ethylene	2.98		*c*
propagation	propylene	propylene	0.014	39	*d*
propagation	propylene	ethylene	0.668	39	*d*
propagation	ethylene	propylene	0.214	39	*d*
propagation	ethylene	ethylene	2.98	39	*d*
chat-agent	propylene	hydrogen	0.088	32	
chat-agent	ethylene	hydrogen	0.088	32	
spon-deact	catalyst	−	0.0001	32	
deact-agent	catalyst	tacticity control agent	0.0001		*e*

[a] General units are L/mol·s. [b] Assumed to be equal to that for activation by cocatalyst. [c] Assumed to be equal to that for homopropagation. [d] Evaluated at 70 °C using an Arrhenius expression. [e] Assumed to be equal to that for spontaneous deactivation.

We begin by considering only the reactors that produce homopolymer. This allows us initially to disregard any reactions involving ethylene, thus simplifying the iterative procedure. We fit the rate constants for propylene−propylene propagation and catalyst activation to match the polymer production in all homopolymer reactors. During this iteration, if required, we adjust the max sites parameter to change the sensitivity of the catalyst concentration to production and readjust the propagation and activation parameters. We then adjust the kinetic parameters for atactic propagation to match the isotactic content of the polymer as closely as possible. Next, we fit the kinetic parameters for chain transfer to hydrogen and monomer to match the values of M_n for the homopolymer reactor grades having different hydrogen-to-monomer ratios.

We then move to the reactors that incorporate ethylene. We adjust the propagation parameters involving ethylene to match the ethylene conversions in these reactors. If we match the total production in all reactors, we move on to adjust the chain-transfer parameters involving hydrogen and ethylene to match M_n for the polymer produced in these copolymer reactors. If we do not match the total production in all reactors, we vary the parameters for catalyst deactivation and return to the homopolymer reactors for another iteration loop.

The iterations are complete when the kinetic parameters allow the model to match all simulation targets, except polymer PDI, for all polymer grades. In the next section, we describe the deconvolution of GPC data used to obtain information about the multisite behavior of the catalyst.

4.4.3. Deconvolution of Molecular-Weight-Distribution Data. We use a statistical algorithm developed by Soares and Hamielec,[37] and implemented by Polythink Inc.,[40] to deconvolute the polymer MWD obtained by gel-permeation chromatography (GPC).

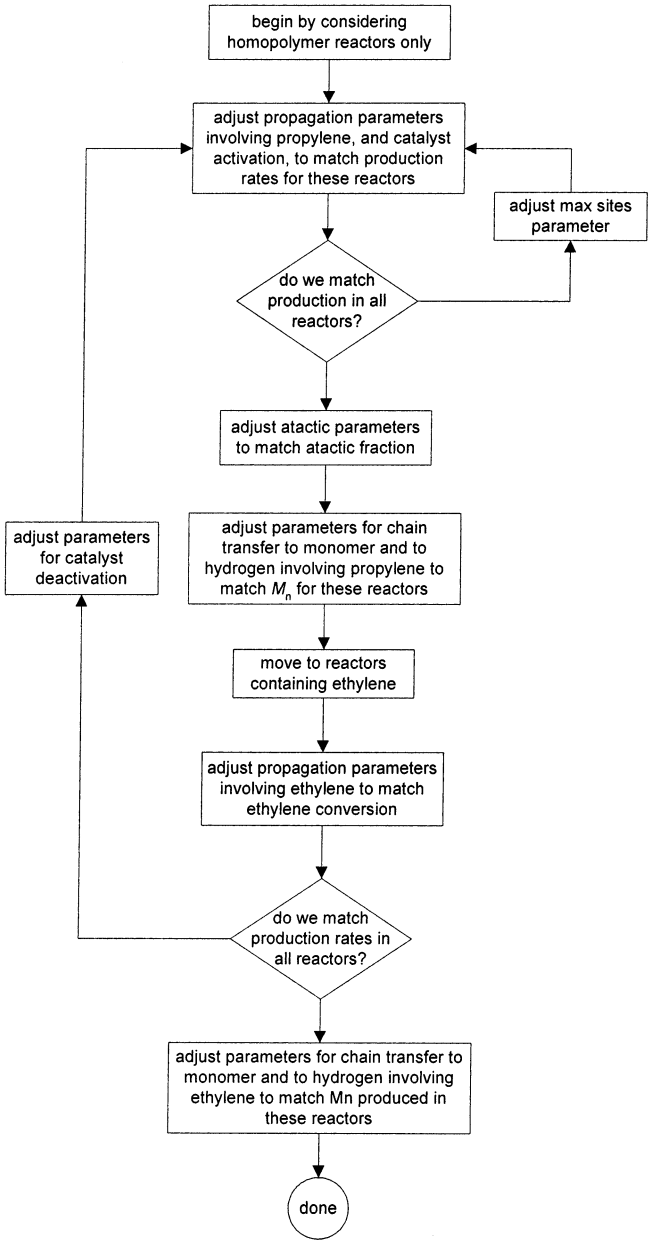

Figure 15. Iterative methodology used to determine kinetic parameters for the single-site model.

This procedure determines the minimum number of site types needed to describe the polypropylene MWD accurately. It is assumed that each site type produces a most-probable MWD. The algorithm also determines the polymer mass fraction and M_n for the polymer produced by each site type.

Soares and Hamielec expressed the most-probable weight chain-length distribution produced by each site type as

$$w_i(n) = \tau_i^2 n \exp(-\tau_i n) \tag{38}$$

where $w_i(n)$ is the weight fraction of polymer of chain length n produced at site type i and τ_i is a fitting parameter for site type i. τ_i represents the inverse of the polymer number-average molecular weight (M_n) produced at site type i. The chain-length distribution of the composite polymer is the sum of these distributions weighted by the mass fractions of polymer produced at each site type

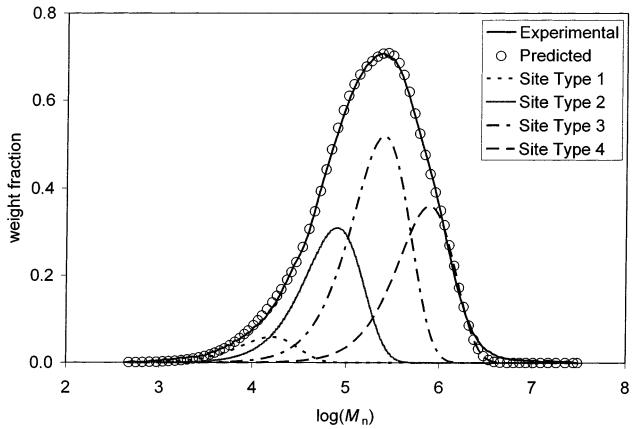

Figure 16. Representative MWD and deconvolution results indicating that a four-site kinetic model is sufficient.

Table 8. Deconvolution Results for a Representative Polypropylene Sample

site type	polymer weight fraction	τ_i (M_n^{-1})	τ_i^{-1} (M_n)
1	0.046 95	1.2459×10^{-4}	8026
2	0.248 27	2.5198×10^{-5}	39 686
3	0.416 27	8.0231×10^{-6}	124 640
4	0.288 52	2.6116×10^{-6}	382 907

$$W(n) = \sum_{i=1}^{j} m_i w_i(n) \tag{39}$$

where $W(n)$ is the total weight fraction of polymer of chain length n, m_i is the mass fraction of polymer produced at site type i, and j is the total number of site types.

Table 8 presents a representative set of deconvolution results for polypropylene. Figure 16 shows the corresponding experimental MWD distribution and the computed results. The algorithm indicates that a four-site model accurately describes the MWD of the polymer. The next section describes the development of the multisite model.

4.4.4. Multisite Kinetic Model. Upon establishing kinetic parameters that allow the single-site model to match all of the respective simulation targets listed in Table 6, we introduce multiple catalyst site types into the process model. The previous section describes the use of a GPC-deconvolution algorithm to determine the optimal number of site types. The deconvolution results also provide two additional simulation targets for the multisite model. These include the mass fraction of polymer and the M_n of the polymer produced by each site type.

We obtain initial values for the propagation rate constants for each catalyst site type by multiplying the rate constant from the single-site model by the mass fraction of polymer produced at each corresponding site type

$$k_{p,i}^{ij} = n_{st} k_p^{ij} m_i \tag{40}$$

where n_{st} is the total number of catalyst site types. We must multiply the rate constant by the number of site types because the total concentration of all site types is n_{st} times the concentration of the individual site types.

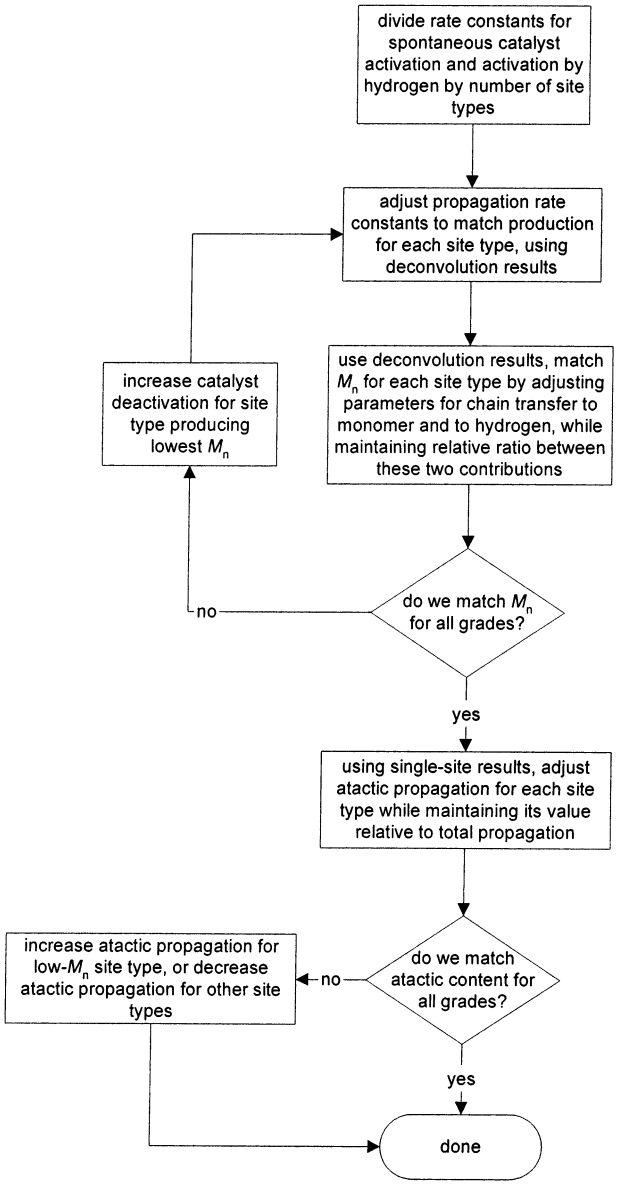

Figure 17. Iterative methodology used to adjust the kinetic parameters in the multisite model.

By using this multiplying factor, we maintain the same total number of catalyst sites between the single-site and multisite models. Note that we assume that the catalyst contains an equal number of moles of each site type. To match the M_n of the polymer produced by each site type, we adjust the rate constants for chain transfer to monomer and to hydrogen.

Figure 17 shows the iterative scheme used to adjust the kinetic parameters in the multisite model. In the model, the concentration of potential sites (CAT) is the same between the single-site and multisite models, but the concentration of vacant sites ($P_{0,i}$) must be divided by the number of site types. We resolve this issue by dividing both the rate constants for catalyst activation by cocatalyst and catalyst activation by hydrogen by the number of catalyst site types. We then use the deconvolution results and eq 38 to set the propagation rate constants to match the mass fraction of polymer produced at each site type. Next, we adjust the rate constants for chain transfer to hydrogen and to monomer to match the M_n of the polymer produced by each site type. We maintain the same relative contributions of chain transfer to hydrogen and to monomer from the single-site model, so that we do not disrupt the sensitivity of these reactions to the concentrations of hydrogen and monomer. This ratio also permits the model to match the molecular weight and PDI for different hydrogen concentrations. If the observed data show an increase or decrease in molecular weight or PDI as the hydrogen concentration changes, changing these ratios allows the model to capture the observed phenomena.

If we do not match M_n for all reactors, we increase the rate constant for deactivation by the tacticity control agent of the catalyst site type that produces polymer of the lowest M_n. As mentioned in section 4.2.5, the tacticity control agent is understood to deactivate some of the site types that produce atactic polymer. Furthermore, atactic polymer that dissolves in solvent is mostly low-molecular-weight species. We return to the step for adjusting propagation rate constants for each site type. We repeat this loop until we match the production rate and the M_n of the polymer produced by each site type.

As initial guesses, we set the rate constant for atactic propagation for each site type such that the ratio of isotactic to total propagation is the same as that for the single-site model. If we do not match the isotactic content for the polymer produced in each reactor, we increase the atactic propagation constant for the low-M_n site type and make a downward adjustment for the remaining site types while maintaining their relative ratios.

5. Dynamic Modeling

5.1. Introduction. A dynamic model allows us to track changes in process variables and other disturbances as a function of time. Such models can be useful for determining the time required for a particular change to propagate through a process or for planning and optimizing grade-change operations. Our aim is to illustrate the utility of a dynamic model by simulating a grade-change operation. In section 5.2, we present a general control scheme for the polypropylene process. In section 6.2, we describe the simulation and present the results.

We create a dynamic model by exporting a steady-state model from Polymers Plus into Aspen Dynamics. We provide additional information not required for steady-state simulation, such as vessel dimensions and geometries, to properly account for the hold-up in each vessel.

5.2. Control Scheme. We investigate a conceptual control scheme and its effect on grade changes. Figure 18 displays a schematic. We include the following controllers in the model:

1. A level controller adjusts the flow of solids out of the reactor to maintain a constant powder level inside the reactor. Because we consider the solid polymer as a condensed phase, this level controller maintains the condensed-phase level in the reactor.

2. A temperature controller adjusts the flow rate of liquid recycle returning to the reactor to maintain the reactor temperature.

3. A pressure controller adjusts the flow rate of cooling medium to the overhead condenser to maintain the reactor pressure.

4. A flow controller adjusts the amount of vapor recycled to the reactor to maintain the ratio of vapor to liquid recycle.

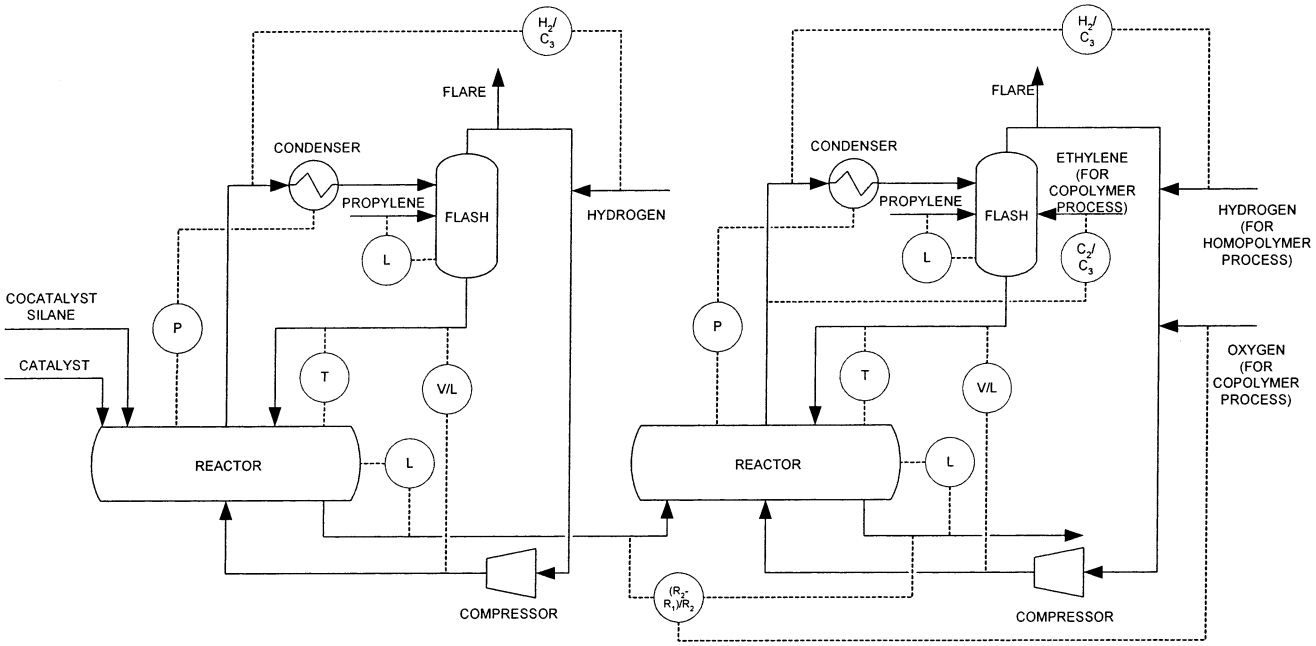

Figure 18. Conceptual control scheme used to simulate a grade change.

Table 9. Controlled and Manipulated Variables in the Control Scheme

controlled variable	manipulated variable
reactor solids level	solids outlet flow
reactor temperature	cooling medium flow
reactor pressure	liquid recycle flow
vapor/liquid recycle ratio	vapor recycle flow
hydrogen/propylene overhead ratio	hydrogen feed rate
flash unit liquid level	propylene feed rate
production in second reactoe	oxygen feed rate

5. A flow controller adjusts the feed rate of hydrogen to maintain a constant ratio of hydrogen to propylene in the reactor off-gas.

6. A level controller adjusts the feed rate of propylene to the overhead flash vessel.

7. A flow controller adjusts the feed rate of oxygen to the second reactor to deactivate the catalyst and subsequently control the production rate relative to that for the first reactor.

Table 9 summarizes the adjusted and manipulated variables.

6. Simulation Results

6.1. Model Validation. We validate the model using steady-state data from four polymer grades produced in a commercial gas-phase polypropylene plant. Two grades are homopolymer and two grades are impact polymer with ethylene as the comonomer. We use these data to develop the polymerization kinetic parameters. Consequently, we can expect the model accuracy to be generally limited to conditions close to those of the four grades.

Figures 19−23 compare simulation results to plant data for the polypropylene production rate, M_n, polydispersity index, atactic content, and reactor mass holdup, respectively. The model matches these process variables very well.

6.2. Model Application. We illustrate the utility of the dynamic model by comparing two grade-transition strategies. Companies often produce several grades of polymer using a single production train. Effective grade-transition policies are therefore required to minimize the transition time and amount of off-specification polymer produced.[41] A basic strategy is to use automatic (proportional-integral, or PI) control to adjust the process variables to meet the targets of the new grade. More aggressive strategies include (1) overshoot, which combines both manual and automatic manipulations of

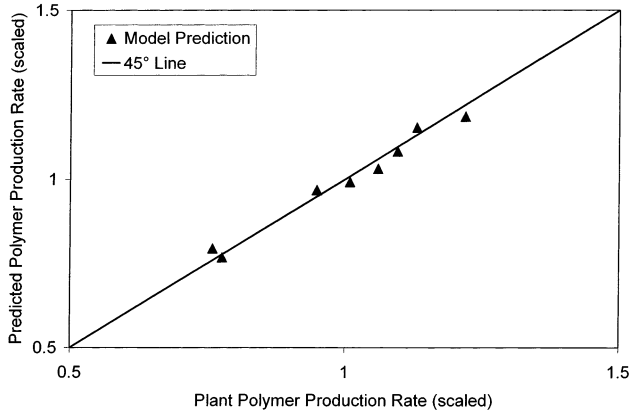

Figure 19. Comparison of model predictions with plant data for the polypropylene production rate.

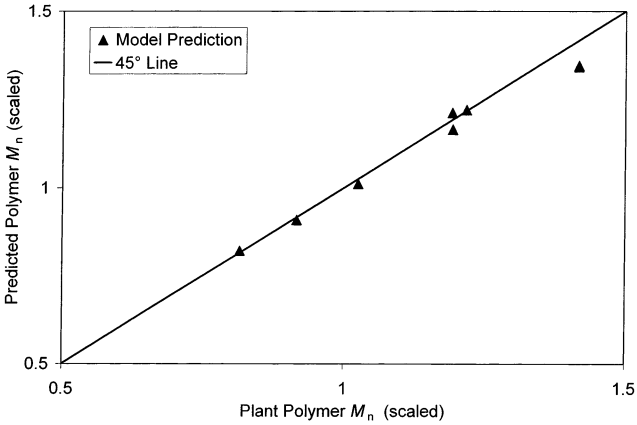

Figure 20. Comparison of model predictions with plant data for the polypropylene M_n.

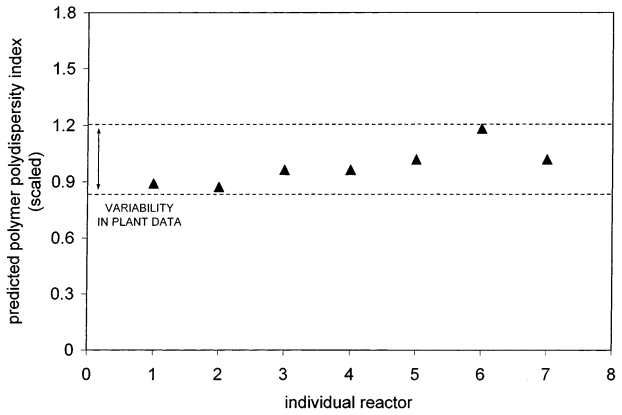

Figure 21. Illustration of model predictions for the polypropylene polydispersity index.

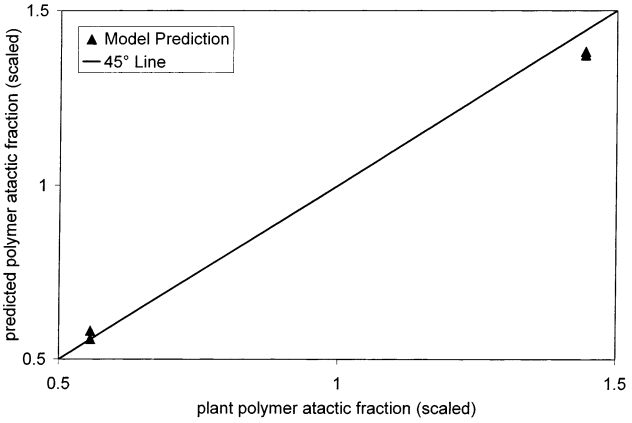

Figure 22. Comparison of model results with plant data for the polypropylene atactic fraction.

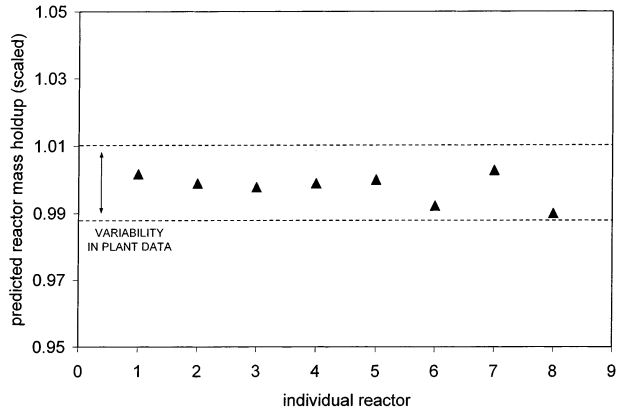

Figure 23. Illustration of model results for the reactor mass holdup.

process variables to reach the target values more rapidly, and (2) de-inventorying, where the reactors are partially emptied to reduce the amount of off-specification polymer produced during the grade change. It is also possible to apply dynamic optimization that can determine the optimal grade-transition profile to minimize the transition time or production of off-specification material. Good strategies can result in significant savings for a given grade change.

As an example, we compare the automatic and overshoot strategies. We use the conceptual control scheme described in section 5.2. Our grade change involves a 10% reduction of the polymer M_n by increasing the amount of fresh hydrogen feed. In the model,

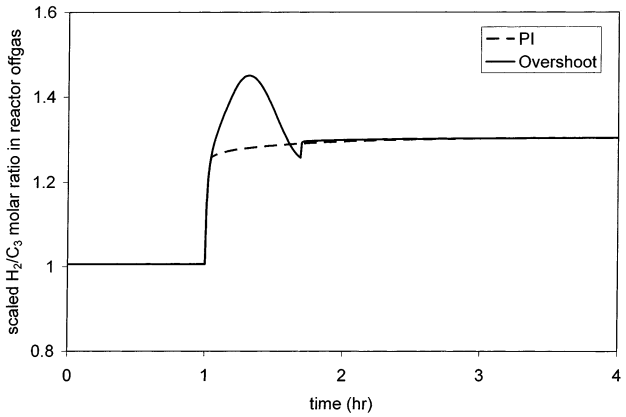

Figure 24. Comparison of the off-gas hydrogen/propylene ratio for the PI and overshoot grade-transition strategies.

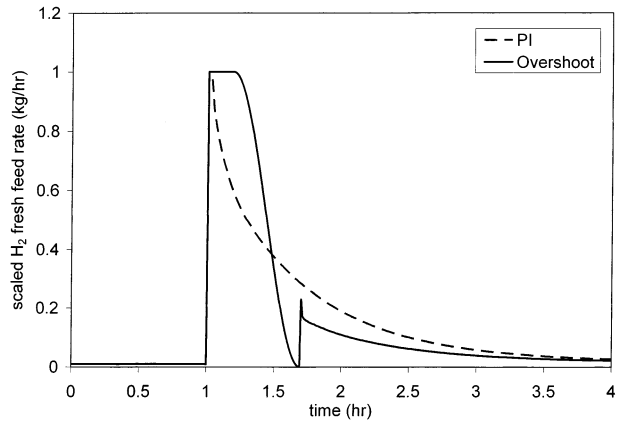

Figure 25. Comparison of the hydrogen fresh feed rate for the PI and overshoot grade-transition strategies.

we achieve the new M_n by increasing the set point for the H_2/C_3 ratio in the reactor off-gas. We consider the polymer to be acceptable when its M_n is within 1% of the new target M_n.

In the first case, we change the set point for the ratio of hydrogen to propylene in the reactor off-gas to the new value and allow the flow controller to automatically manipulate the hydrogen feed rate to meet the new target value. In the second case, we employ an overshoot strategy, whereby we manually increase the hydrogen feed rate until we exceed the target ratio of hydrogen to propylene. When the off-gas ratio approaches the desired target, we then switch the controller to automatic and allow it to settle out at the new value.

Figures 24 and 25 compare the off-gas H_2/C_3 ratio and the hydrogen fresh feed rate, respectively, for the PI and overshoot strategies. Under the automatic control strategy, the hydrogen flow controller initially increases its flow to the maximum value and then gradually reduces it to meet the new set point for the off-gas composition. In the overshoot strategy, we keep the hydrogen flow at its maximum value for a longer period of time, causing the model to overshoot the set point for the off-gas composition.

Figure 26 compares the resulting polypropylene M_n for the PI and overshoot strategies. The overshoot strategy achieves the target M_n, within the acceptable error, in 1.8 h, whereas the PI strategy reaches the target M_n in 2.7 h. The overshoot strategy allows the transition to take place 33% faster. This also corresponds to a 38% reduction in off-specification polymer produced during the grade change.

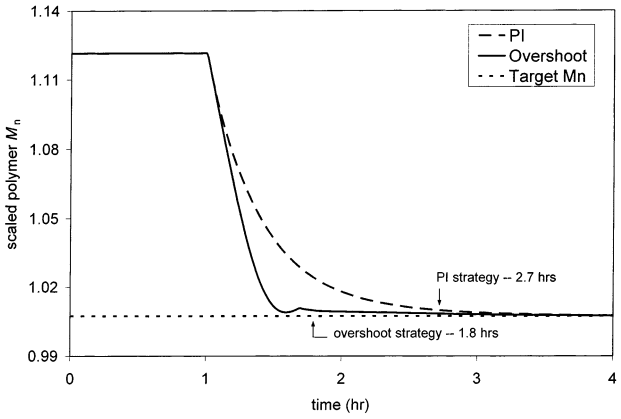

Figure 26. Comparison of the polypropylene M_n for the PI and overshoot grade-transition strategies.

7. Conclusions

The PC−SAFT EOS does an excellent job of describing the physical and thermodynamic properties and phase equilibrium for the gas-phase polypropylene process. One can represent the behavior of the horizontal stirred-bed reactors using four CSTRs configured in series. One can describe the Ziegler−Natta catalyst used for polypropylene production by assuming the existence of multiple catalyst site types, each with its own relative reactivity. The steady-state model accurately predicts the major polymer properties and key process variables for four polymer trains. The model reliability is generally limited to systems whose feed compositions and process conditions are close to those used in model validation.

Several unique challenges were encountered during this modeling project. There were different stakeholders in the project, with different modeling objectives. We agreed to a common methodology and success criteria before the modeling began. Project communication was an issue, because teams were based in different geographical locations. This required effective project management techniques. There is always a desire to model everything in the plant. However, modeling is an art of simplifying the complexity while still capturing the essential details.

A validated model, such as the one presented here, generates value for companies. It permits the exploration of different feed rates and operating conditions without wasting raw material or manpower. One can use the model to debottleneck the process, test new catalysts and products, and design new polymer grades. Finally, we can use the dynamic model to explore various grade-change strategies, to minimize the transition time and the production of off-specification polymer.

Acknowledgment

We thank Alliant Techsystems, Aspen Technology (particularly, Dustin MacNeil, Director of Worldwide University Programs; Larry Evans, Board Chairman), China Petroleum and Chemical Corporation (particularly Xianghong Cao, Senior Vice President), and Honeywell Specialty Materials and Honeywell International Foundation for supporting the educational programs in computer-aided design and process systems engineering at Virginia Tech.

Symbols

English Symbols

A = parameter in the polynomial for the ideal-gas heat capacity, J/kmol·K
a^{res} = molar residual Helmholtz energy, J/kmol
a^{ref} = reference contribution to the molar residual Helmholtz energy in the PC−SAFT EOS, J/kmol
a^{pert} = perturbation contribution to the molar residual Helmholtz energy in the PC−SAFT EOS, J/kmol
B = parameter in the polynomial for the ideal-gas heat capacity, J/kmol·K^2
C = parameter in the polynomial for the ideal-gas heat capacity, J/kmol·K^3
C_p = constant-pressure heat capacity, J/kmol·K
C_p^{ig} = constant-pressure ideal-gas heat capacity, J/kmol·K
ΔC_p = EOS contribution to the heat capacity, J/kmol·K
CAT_i = inactive catalyst site of type i
COCAT = cocatalyst
CSTR = continuous stirred-tank reactor
D = parameter in the polynomial for the ideal-gas heat capacity, J/kmol·K^4
D_n = inactive polymer chain containing n monomer segments
$[D_n]$ = concentration of inactive polymer chains containing n monomer segments, mol/L
$DCAT_i$ = deactivated catalyst site of type i
EOS = equation of state
GPC = gel permeation chromatography
H_i^l = liquid enthalpy for species i, J/kmol
H_i^v = vapor enthalpy for species i, J/kmol
ΔH_f = heat of propylene polymerization, kcal/mol
ΔH_i^{vap} = heat of vaporization for species i, kJ/kg
HDPE = high-density polyethylene
k = rate constant with general units of L/mol·s
$k_{act,i}$ = rate constant for activation of catalyst site type i, L/mol·s
$k_{acth,i}$ = rate constant for activation by hydrogen of catalyst site type i, L/mol·s
k_B = Boltzmann constant, 1.38×10^{-23} J/K
$k_{ds,i}$ = rate constant for spontaneous deactivation of catalyst site type i, s^{-1}
$k_{dtca,i}$ = rate constant for deactivation of catalyst site type i by tacticity control agent, L/mol·s
$k_{ini,i}$ = rate constant for chain initiation of site type i, L/mol·s
$k_{ini,i}^j$ = rate constant for chain initiation of site type i by monomer type j, L/mol·s
$k_{p,i}$ = rate constant for total chain propagation for catalyst site type i, L/mol·s
$k_{p,i}^{jk}$ = rate constant for total chain propagation for monomer type j adding to segment type k for a chain attached to catalyst site type i, L/mol·s
$k_{pa,i}$ = rate constant for atactic chain propagation for catalyst site type i, L/mol·s
$k_{th,i}$ = rate constant for chain transfer to hydrogen for catalyst site type i, L/mol·s
$k_{th,i}^j$ = rate constant for chain transfer to hydrogen for a chain ending in segment type j, attached to catalyst site type i, L/mol·s
$k_{tm,i}$ = rate constant for chain transfer to monomer for catalyst site type i, L/mol·s
$k_{tm,i}^{jk}$ = rate constant for chain transfer to monomer type j for a chain ending in segment type k, attached to catalyst site type i, L/mol·s
m = characteristic chain length for conventional species in the PC−SAFT EOS
m_i = mass fraction of polymer produced at catalyst site type i
M = monomer

M_i = monomer of type i
M_n = number-average molecular weight, g/mol
M_w = weight-average molecular weight, g/mol
MW_{seg} = segment molecular weight, g/mol
MWD = molecular-weight distribution
n = number of monomer segments in the polymer (degree of polymerization)
n_{st} = number of catalyst site types
P = pressure, bar
$P_{0,i}$ = activated catalyst site of type i
$P_{1,i}$ = initiated catalyst site of type i
$P^j_{1,i}$ = initiated polymer chain containing segment type j attached to catalyst site type i
P_c = critical pressure, bar
$P_{n,i}$ = live polymer chain containing n segments attached to catalyst site type i
$P^j_{n,i}$ = live polymer chain containing n segments attached to catalyst site type i ending in segment type j
PDI = polymer polydispersity index
$[P_n]$ = concentration of active polymer chains containing n monomer segments, mol/L
PC−SAFT = perturbed-chain statistical associating fluid theory equation of state
r = size parameter for polymer species in the PC−SAFT EOS; ratio of the characteristic chain length to the number-average molecular weight, mol/g
RTD = residence time distribution
SAFT = statistical associating fluid theory equation of state
T = temperature, °C
T_c = critical temperature, °C
TCA = tacticity control agent
V = volume, L
VLE = vapor−liquid equilibrium
$w_i(n)$ = weight fraction of chains of length n produced at catalyst site type i
$W(n)$ = total weight fraction of chains containing n segments
z = compressibility
z^{id} = ideal contribution to the compressibility in the PC−SAFT EOS, equal to unity
z^{ref} = reference contribution to the compressibility in the PC−SAFT EOS
z^{pert} = perturbation contribution to the compressibility in the PC−SAFT EOS

Greek Symbols

ϵ = segment energy parameter in the PC−SAFT EOS, J
λ_i = ith moment for all polymer chains
μ_i = ith moment for active polymer chains
σ = segment characteristic diameter in the PC−SAFT EOS, Å
τ = residence time, h
τ_i = adjustable parameter for the chain length distribution function, mol/g

Literature Cited

(1) Choi, K. Y.; Ray, W. H. The Dynamic Behavior of Continuous Stirred-Bed Reactors for the Solid Catalyzed Gas Phase Polymerization of Propylene. *Chem. Eng. Sci.* **1988**, *43*, 2587.

(2) McAuley, K. B.; MacDonald, D. A.; McLellan, P. J. Effects of Operating Conditions on Stability of Gas-Phase Polyethylene Reactors. *AIChE J.* **1995**, *41*, 868.

(3) Choi, K. Y. Gas-Phase Olefin Polymerization. In *Polymeric Materials Encyclopedia*; Salamone, J. C., Ed.; CRC Press: Boca Raton, FL, 1996; p 2707.

(4) Shepard, J. W.; Jezl, J. L.; Peters, E. F.; Hall, R. D. Divided Horizontal Reactor for the Vapor Phase Polymerization of Monomers at Different Hydrogen Levels. U.S. Patent 3,957,488, 1976.

(5) Jezl, J. L.; Peters, E. F.; Hall, R. D.; Shepard, J. W. Process for the Vapor Phase Polymerization of Monomers in a Horizontal, Quench-Cooled, Stirred-Bed Reactor Using Essentially Total Off-Gas Recycle and Melt Finishing. U.S. Patent 3,965,083, 1976.

(6) Peters, E. F.; Spangler, M. J.; Michaels, G. O.; Jezl, J. L. Vapor Phase Reactor Off-Gas Recycle System for Use in the Vapor State Polymerization of Monomers. U.S. Patent 3,971,768, 1976.

(7) Jezl, J. L.; Peters, E. F. Horizontal Reactor for the Vapor Phase Polymerization of Monomers. U.S. Patent 4,129,701, 1978.

(8) Kissel, W. J.; Han, J. H.; Meyer, J. A. Polypropylene: Structure, Properties, Manufacturing Processes, and Applications. In *Handbook of Polypropylene and Polypropylene Composites*; Karian, H. G., Ed.; Marcel Dekker: New York, 1999; p 15.

(9) Caracotsios, M.; Theoretical Modelling of Amoco's Gas-Phase Horizontal Stirred Bed Reactor for the Manufacturing of Polypropylene Resins. *Chem. Eng. Sci.* **1992**, *47*, 2591−2596.

(10) Moore, E. P. Polypropylene (Commercial). In *Polymeric Materials Encyclopedia*; Salamone, J. C., Ed.; CRC Press: Boca Raton, FL, 1996; p 6578.

(11) Seppälä, J. V.; Härkönen, M.; Luciani, L.; Effect of the Structure of External Alkoxysilane Donors on the Polymerization of Propene with High Activity Ziegler−Natta Catalysts. *Makromol. Chem.* **1989**, *190*, 2535.

(12) Balow, M. J. Growth of Polypropylene Usage as a Cost-Effective Replacement of Engineering Polymers. In *Handbook of Polypropylene and Polypropylene Composites*; Karian, H. G., Ed.; Marcel Dekker: New York, 1999; p 1.

(13) Zacca, J. J.; Debling, J. A.; Ray, W. H.; Reactor Residence Time Distribution Effects on the Multistage Polymerization of Olefins − I. Basic Principles and Illustrative Examples, Polypropylene. *Chem. Eng. Sci.* **1996**, *51*, 4859.

(14) Gross, J.; Sadowski, G.; Perturbed-Chain SAFT: An Equation of State Based on a Perturbation Theory for Chain Molecules. *Ind. Eng. Chem. Res.* **2001**, *40*, 1244.

(15) Chapman, W. G., Gubbins, K. E.; Jackson, G.; Radosz, M. New Reference Equation of State for Associating Liquids. *Ind. Eng. Chem. Res.* **1990**, *29*, 1709.

(16) Huang, S. H.; Radosz, M. Equation of State for Small, Large, Polydisperse, and Associating Molecules. *Ind. Eng. Chem. Res.* **1990**, *29*, 2284.

(17) Huang, S. H.; Radosz, M. Equation of State for Small, Large, Polydisperse, and Associating Molecules: Extension to Fluid Mixtures. *Ind. Eng. Chem. Res.* **1991**, *30*, 1994.

(18) *DIPPR Online Database*; Design Institute for Physical Properties, American Institute of Chemical Engineers (AIChE): New York, 2001.

(19) Sychev, V. V.; Vasserman, A. A.; Golovsky, E. A.; Kozlov, A. D.; Spiridonov, G. A.; Tsymarny, V. A. *Thermodynamic Properties of Ethylene*; Hemisphere Publishing Corp.: Washington, DC, 1987.

(20) Zoller, P. Pressure−Volume−Temperature Relationships of Solid and Molten Polypropylene and Poly(butene-1). *J. Appl. Polym. Sci.* **1979**, *23*, 1057.

(21) Gaur, U.; Wunderlich, B. Heat Capacity and Other Thermodynamic Properties of Linear Macromolecules. IV. Polypropylene. *J. Phys. Chem. Ref. Data* **1981**, *10*, 1051.

(22) Smith, J. M.; Van Ness, H. C. *Introduction to Chemical Engineering Thermodynamics*, 4th ed.; McGraw-Hill: New York, 1987; p 571.

(23) Poling, B. E.; Prausnitz, J. M.; O'Connell, J. P. *The Properties of Gases and Liquids*, 5th ed.; McGraw-Hill: New York, 2001.

(24) Gaur, U.; Wunderlich, B. Heat Capacity and Other Thermodynamic Properties of Linear Macromolecules. II. Polyethylene. *J. Phys. Chem. Ref. Data* **1981**, *10*, 119.

(25) Beaton, C. F.; Hewitt, G. F. *Physical Property Data for the Design Engineer*; Hemisphere Publishing Corp.: New York, 1989.

(26) Ohgaki, K.; Nakai, S.; Nitta, S.; Katayama, T. Isothermal Vapor−Liquid Equilibria for the Binary Systems Propylene−Carbon Dioxide, Propylene−Ethylene and Propylene−Ethane at High Pressure. *Fluid Phase Equilib.* **1982**, *8*, 113.

(27) Williams, R. B.; Katz, D. L. Vapor−Liquid Equilibria in Binary Systems. Hydrogen with Ethylene, Ethane, Propylene, and Propane. *Ind. Eng. Chem.* **1954**, *46*, 2512.

(28) Leonard, J. Heats and Entropies of Polymerization, Ceiling Temperatures, Equilibrium Monomer Concentrations, and Polymerizability of Heterocyclic Compounds. In *Polymer Handbook*; Brandrup, J., Immergut, E. H., Grulke, E. A., Eds.; Wiley & Sons: New York, 1999; p II/363.

(29) Arriola, D. J. Modeling of Addition Polymerization Systems. Ph.D. Dissertation, University of Wisconsin, Madison, WI, 1989.

(30) Levenspiel, O. *Chemical Reaction Engineering*; John Wiley & Sons: New York, 1972.

(31) Nagel, E. J.; Kirillov, V. A.; Ray, W. H. Prediction of Molecular Weight Distributions for High-Density Polyolefins. *Ind. Eng. Chem. Prod. Res. Dev.* **1980**, *19*, 372.

(32) McAuley, K. B.; MacGregor, J. F.; Hamielec, A. E. A Kinetic Model for Industrial Gas-Phase Ethylene Copolymerization. *AIChE J.* **1990**, *36*, 837.

(33) Xie, T.; McAuley, K. B.; Hsu, J. C. C.; Bacon, D. W. Gas-Phase Ethylene Polymerization: Production Processes, Polymer Properties, and Reactor Modeling. *Ind. Eng. Chem. Res.* **1994**, *33*, 449.

(34) Cansell, F.; Siove, A.; Fontanille, M. Ethylene-Propylene Copolymerization Initiated with Solubilized Ziegler−Natta Macromolecular Complexes. I. Determination of Kinetic Parameters. *J. Polym. Sci. A: Polym. Chem.* **1987**, *25*, 675.

(35) Kissin, Y. V. *Isospecific Polymerization of Olefins with Heterogeneous Ziegler−Natta Catalysts*; Springer-Verlag: New York, 1985.

(36) Kissin, Y. V. Multicenter Nature of Titanium-Based Ziegler−Natta Catalysts: Comparison of Ethylene and Propylene Polymerization Reactions. *J. Polym. Sci. A: Polym. Chem.* **2003**, *41*, 1745.

(37) Soares, J. B. P.; Hamielec, A. E. Deconvolution of Chain-Length Distributions of Linear Polymers Made by Multiple-Site-Type Catalysts. *Polymer* **1995**, *36*, 2257.

(38) Khare, N. P.; Seavey, K. C.; Liu, Y. A.; Ramanathan, S.; Lingard, S.; Chen, C.-C. Steady-State and Dynamic Modeling of Commercial Slurry High-Density Polyethylene (HDPE) Processes. *Ind. Eng. Chem. Res.* **2002**, *41*, 5601.

(39) Ma, Q.; Wang, W.; Feng, L.; Wang, K.; Studies on Kinetics of Ethylene−Propylene Gas-Phase Copolymerization. *Gaofenzi Xuebao* **2001**, *6*, 746−750.

(40) Polythink Inc., 1005 Sydenham Rd., S.W., Calgary, Alberta, Canada T2T 0T3. http://www.polythink.com (accessed August 2002).

(41) Debling, J. A.; Han, G. C.; Kuijpers, F.; VerBurg, J.; Zacca, J.; Ray, W. H. Dynamic Modeling of Product Grade Transitions for Olefin Polymerization Processes. *AIChE J.* **1994**, *40*, 506.

Received for review September 15, 2003
Revised manuscript received December 10, 2003
Accepted December 17, 2003

IE030714T